

TARGET IDENTIFICATION AND DELTA-V SIZING FOR ACTIVE DEBRIS REMOVAL AND IMPROVED TRACKING CAMPAIGNS

Glenn E. Peterson

Senior Engineering Specialist, Astrodynamics Department, The Aerospace Corporation,
P.O. Box 92957, Los Angeles, CA 90009-2957, 310-336-1904, glenn.e.peterson@aero.org

Abstract: Long-term projections of the low Earth orbit debris environment show the number of objects is increasing, even in the event of no future launches. Various proposals have been made to mitigate the growth including actively removing objects from orbit or tracking currently orbiting objects to a greater degree of precision to facilitate more effective risk assessment. However, the cost of single removal or tracking missions is most likely prohibitive. An alternative is for a single mission to engage multiple targets. This paper determines desirable targets for such missions in terms of likelihood of future debris production and sizing of deltaV requirements.

Keywords: Orbital debris, active debris removal, mission planning

1. Introduction

The Aerospace Corporation, under the auspices of the United States Air Force (USAF) developmental planning and architectures group (SMC/XRD), recently performed modeling of the future growth of the space debris environment in Low Earth Orbit (LEO)¹. Studies of the results indicated that some of the consequences of the projected growth include an expected 3 to 18% increase in the cost of space missions due to reliability degradation of orbiting assets by 2050², increased number of collision avoidance alerts^{3,4}, and increased likelihood of launch windows being closed³. Other studies have shown that missions that actively remove debris-producing objects can reduce the rate of debris growth⁵ and that tracking objects with a higher degree of fidelity can reduce the number of collision avoidance (COLA) alerts⁴.

One of the difficulties in performing debris risk reduction missions is that spacecraft and launch vehicles are expensive. In order to make a mission worthwhile, the benefit (i.e., the effectiveness of the mission) must outweigh the cost. One way to reduce the cost is to launch missions that have multiple targets. For example, a large orbit transfer vehicle (OTV) capable of moving between targets would be used to deploy mini-satellites (like 3U CubeSats), which could either be placed on or very near a selected target. The mini-satellite could then attach itself to the target and deploy a drag-enhancement device, or fly in proximity to the target, use relative ranging, and thereby act as a beacon to allow for high precision tracking⁶. In this study, desirable target objects for active debris removal (ADR) or tracking missions are identified based upon the statistical results of the recent modeling effort along with the delta-V requirements to move

between the targets in an efficient manner. An on-orbit vehicle was assumed that has either an impulsive or low-thrust delta-V capability commensurate with proposed systems when traveling from target to target.

2. Current Catalog Object Composition

The tracked objects in low Earth orbit (LEO) are generally categorized in terms of three groups: satellites (payloads), rocket bodies, and debris. Satellites here refer to any payload that was the purpose of a launch effort and does not necessarily imply the object is currently in an operational status. Rocket bodies are the upper stages left over from a launch effort and are here assumed to be intact. Debris objects are those objects in orbit that are tracked but are neither satellites nor rocket bodies. They are the remnants of collisions, fragmentations, or simply pieces of larger objects that have been shed by the larger parent.

Figure 1, left hand pie chart, shows the breakdown of the satellites in terms of their country of origin. The Commonwealth of Independent States (CIS, formerly the Soviet Union) has the most satellites still in orbit (~58%). This is a reflection of their mission philosophy: quantity vs. quality. Their procedure was to rapidly build inexpensive satellites and then launch on a continual basis. This can be seen when examining a breakdown of the CIS satellites by bus-type. Approximately 35% of the CIS satellites were Strela-1 small communication data-dump satellites. Over 300 of these were placed into orbit until the larger Strela-3 became operational, which itself accounts for 14% of the CIS satellites. The Kaur-1 bus composed 22% of CIS satellites and was used on a multitude of missions (Parus, Tsikada, Nadezdha, Strela-2, and a few smaller scientific satellites). After CIS, the United States is next in size and has contributed ~20% of the satellites in orbit. The US general launch philosophy has been to build fewer (and more unique) but larger and more expensive spacecraft than CIS. The 20% US value shown here excludes the US-based commercial Iridium, Globalstar, and Orbcomm constellations. Together these three comprise about 10% of the satellites in LEO. Europe and Asia have placed much fewer satellites in orbit than either the US or Russia, at least up to the current time.

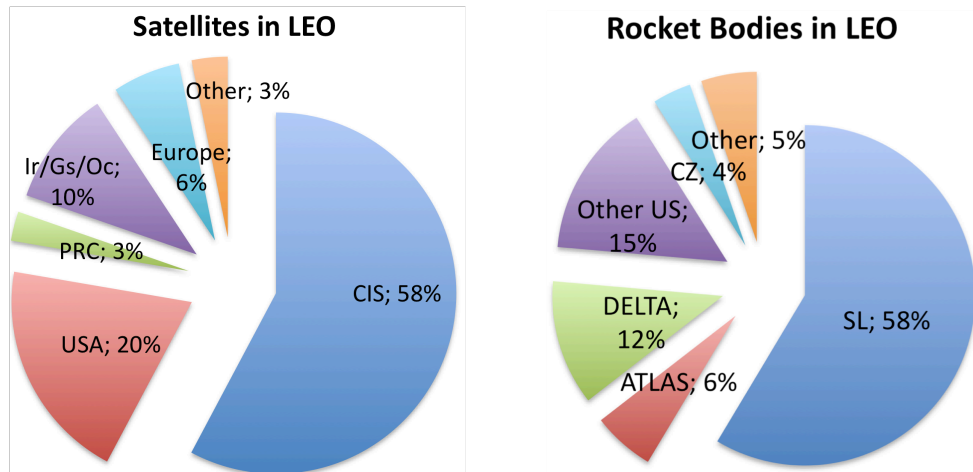


Figure 1: Satellites and rocket bodies (intact objects) in low Earth orbit

Figure 1, right hand pie chart, shows the breakdown of the rocket bodies by launch vehicle type. Their distribution is very similar to the satellites as expected. The Russians utilize the SL-series of launch vehicles whose upper stages comprise ~58% of the orbiting rocket bodies; almost half (~45%) of the SL rocket bodies are of the SL-8 variety. The United States is next with ~33%, with the Delta series of rocket bodies being the largest contributor at 12% and Atlas next with 6%. As with the satellites, European and Asian rocket bodies comprise a smaller portion of the overall total.

Figure 2 shows the breakdown of the debris pieces by origin. The Chinese ASAT test involving Fengyun 1C and the Iridium-33/Cosmos-2251 collisions are broken out separately. Together, these two events make up 44% of the currently orbiting debris. The United States and Russia are roughly equivalent in their “ownership” of tracked debris, but while ~90% of the US debris came from rocket body events, the Russian debris is roughly split between residue from satellites and rocket bodies.

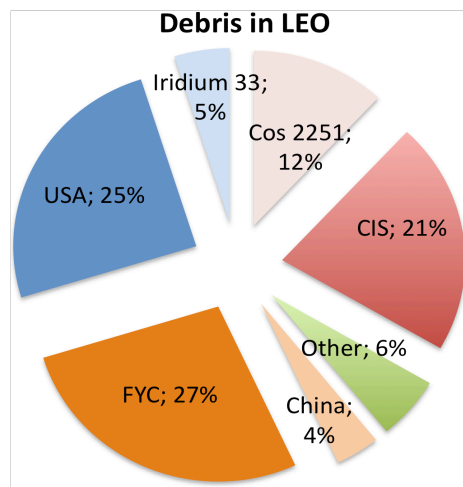


Figure 2: Debris (non-intact objects) in low Earth orbit

Figure 3 shows the orbit element distribution for the large intact objects (satellites and rocket bodies) and the debris in LEO. The intact objects have orbit elements that are tightly constrained in both the semi-major axis and inclination. This reflects the practice of the space community in using and re-using the same orbits over and over. In comparison, the debris objects are much more spread out in altitude due to atmospheric decay but are also tightly constrained in the inclination, albeit slightly less constrained than the intact objects.

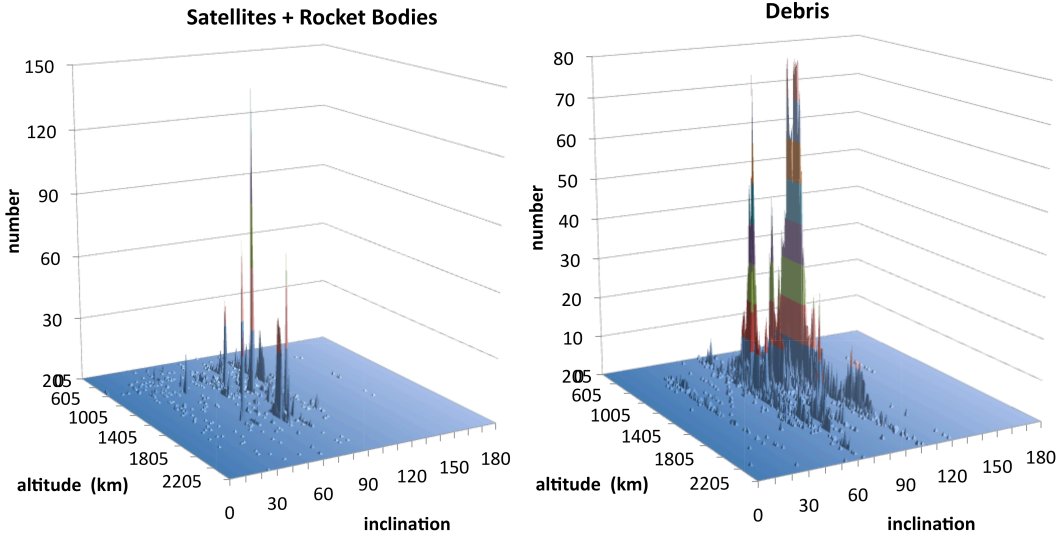


Figure 3: Orbit element distribution of objects in low Earth orbit

3. Debris Model Description

The 100-year projection of the LEO debris environment has been detailed elsewhere^{1,2}, but a summary is warranted here. The model begins with the current public catalog depicted in Figures 1 & 2 (initial starting date of July, 2009), with a mass-law extrapolation to generate the sub-trackable particle sizes (between 1 and 10 cm). The model discretely determines collisions by a Monte Carlo draw between individual objects as the objects are propagated into the future, with new satellites and rocket bodies being added annually based upon replicating the last 10 years of historical activity. When a collision occurs, the resulting debris field is determined by the program IMPACT using the unique orbit and mass properties of the two objects. The new debris pieces are fed back into the simulation as part of the debris population and could conceivably participate in additional collisions.

By treating the objects as discrete entities, identification of those objects that are statistically likely to contribute the most to the growth in the debris population can be determined. These high likelihood objects provide potential targets for either ADR campaigns or increased tracking to enable more efficient collision avoidance of these objects. Analysis of the model results found that collisions between large objects (both in terms of size and mass) were dominant contributors to the future debris environment.

Figure 4 shows the resulting spatial density as derived from the model for objects larger than 10 cm in size (current tracking capability) at three snapshots in time: 2009, 2059, and 2109. In general, the density is expected to increase noticeably over the next 100 years with the growth mostly occurring in the out-years. Peaks occur in the heavily populated low LEO region (~700-900 km) where Sun-synchronous satellites, and Iridium and Orbcomm constellations reside, at ~900-1000 km where the Russian Parus satellites orbit, and at high LEO (~1400 km) where the Globalstar constellation and Russian Strela satellites lie. The results from the 100-year projections¹ indicate that the debris environment is in a state of self-generation and will grow even if there is no future launch activity. This confirms previous studies performed by others⁴.

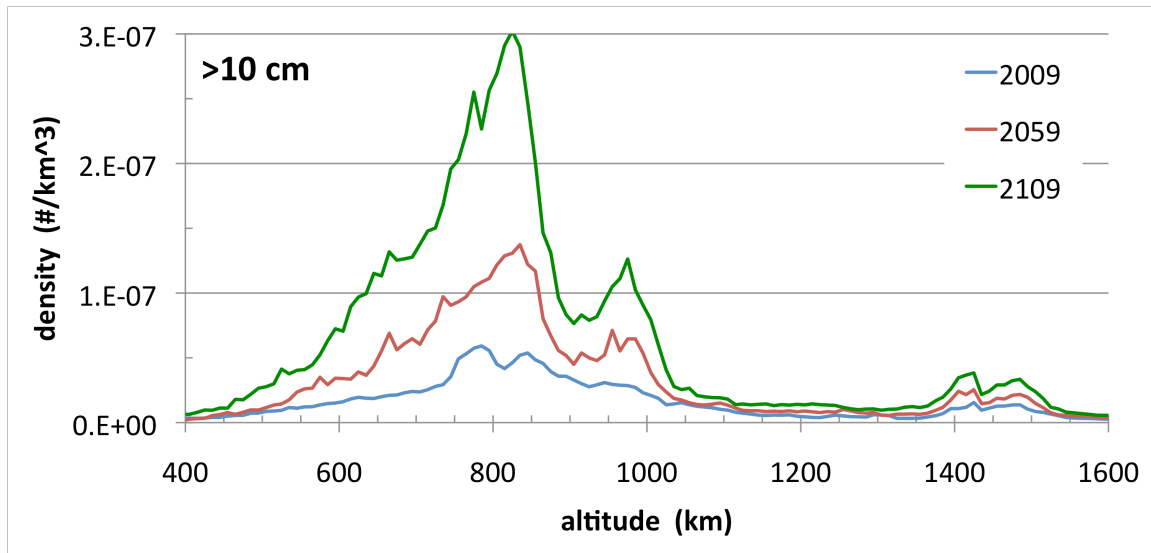


Figure 4. Spatial density from discrete catalogs as a function of altitude

4. Target Object Identification

Target selection for ADR or enhanced tracking missions is problematic. Since there is no way to deterministically know which objects are going to collide in the future, the only way to select reasonable targets is in a probabilistic manner; that is, remove those objects that are most likely to create debris. This likelihood of generating debris is a function of the target’s kinetic energy and probability of collision. The kinetic energy (velocity and mass) is relevant since this determines the extent of fragmentation of the objects when they collide, while the probability of collision (size and spatial density of other objects that it faces given its orbital parameters) expresses the likelihood that the target will collide with some other object. These values can be combined into a “probability-severity” (P-S) parameter that reflects both the target’s likelihood of being in a collision and its propensity to create debris should it be hit.

It was found through the debris modeling process that collisions involving the intact satellites and rocket bodies produce much more debris than collisions involving just the smaller debris objects, even though debris outnumbers the intact objects. Therefore, the best targets will be the large intact objects. In the modeling process, future launch activity replicates the same behavior every 10 years (and is based on the activity from the years 2000-2010). Therefore, intact objects with the same mass are being placed into the same orbits every 10 years. Given that any ADR or tracking mission is assumed to occur at the end of a satellite’s operational phase at 10 years or occurs immediately for rocket bodies, then determining which targets are the “best” for a single 10-year block will approximate to the entire future launch population. Figure 5 ranks the intact objects that will potentially generate the most debris by total fragments created during the simulation averaged over 100 Monte Carlo runs. Larger values on this plot imply a greater combination of likelihood of collision and the severity of the consequences of the collision. These results provide the basis for the “best” targets, but do not contain the entire story.

In addition to the probability-severity listing, the proposed mission examined in this study requires that an on-orbit device be able to perform its function against multiple targets. Therefore,

while P-S is one important parameter, similarity of orbits of the various targets is another. In essence, due to the large delta-Vs that would be required, a multi-target mission could not start with the highest P-S value target, then moved to the second highest target, then to the third, etc. Instead, to maximize the number of accessible targets (i.e., to minimize propellant cost), targets with a high P-S value but also with similar orbits would be the most favorable candidates.

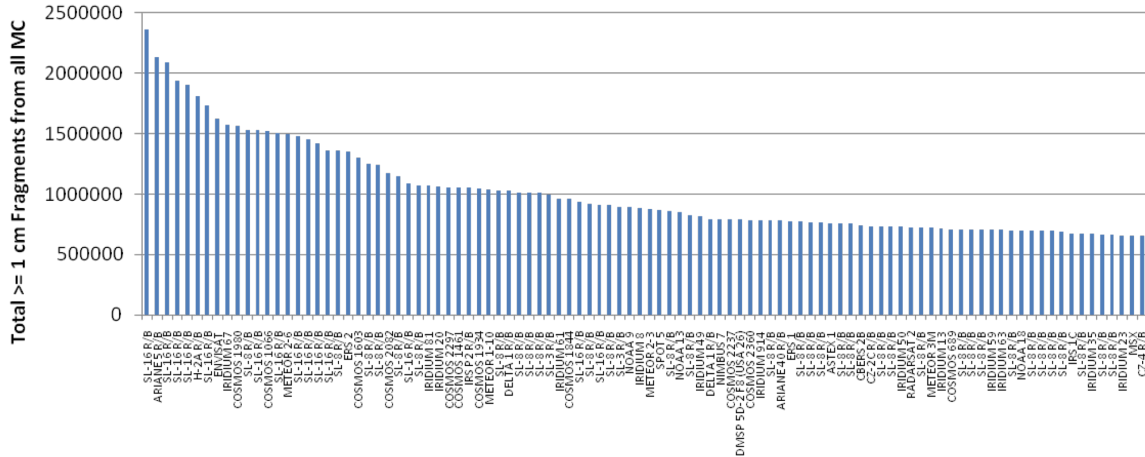


Figure 5: Collision Probability-Severity (P-S parameter), Top 100 Objects

Table 1 lists the intact objects of Figure 5 but have been grouped by similarity of orbit, which implies they could conceivably be reached by a single vehicle. While the objects in Table 1 and Figure 5 are the result of an average of 100 Monte Carlo runs, individual objects that are in the same family of objects can move on and off the top 100 list depending upon the specific Monte Carlo run selected for examination. For example, there are 39 SL-16/Tselina-2 objects (18 SL-16 & 21 Tselina-2) in the public Resident Space Object catalog in a similar orbit, but only 19 of them made the top 100 list. There is no way to know a priori which of the 39 will contribute to the future real-world debris growth and which will not. Therefore, they must be treated as a group when planning missions.

The “best” target group is the SL-16 rocket bodies. At 8300 kg, they are some of most massive objects in orbit and contribute a large amount of debris to the future projections of the LEO debris environment. The SL-8 rocket bodies are next; they are in highly inclined orbits with respect to other objects resulting in high relative velocities, have a significant mass, and there are over 400 of them. There are also a multitude of various types of objects in Sun-synchronous orbit. The most massive are derivatives of the European SPOT buses, the largest being the Envisat satellite with a mass of 8200 kg (three other SPOT bus satellites were in the top 100 list shown in Figure 5). Finally, the Iridium satellites are favorable targets because they are identical and all reside in the same orbit. If control is lost of these vehicles, they will present a significant risk of collision against each other.

Table 1: Most likely debris-generating objects from model simulation

% of mass	Inclination (deg)	Altitude (km)	# (out of 100)	# in catalog	Comments
46	71	835	19	39	SL-16 R/B & Tselina-2
24	~98-99	770-1000	24	189	Sun-synchronous
16	83	980	30	311	Mostly SL-8 R/B
5	81	865	6	58	SL-3 R/B & various satellites
3	74	770	6	100	SL-8 R/B
3	86	780	13	85	Iridium

5. Delta-V Sizing

While the goal of a multi-target debris-related mission is to be able to reach as many targets as possible, fuel constraints limit a maneuvering spacecraft in the number of targets that it can reach. Therefore, when selecting target objects for a debris-related mission, it is beneficial to choose targets that have orbits as similar as possible. Given that plane changes require the largest delta-V, the first step to maximize the number of reachable targets is to pick objects that are in similar inclinations. For example, when examining just the 18 SL-16 rocket bodies in Table 1, they all have similar altitudes and eccentricities, (near zero) while the inclinations range from 70.89 to 71.02 degrees. With similar altitude, eccentricity and inclination, the main orbit element that needs to be adjusted is the right ascension of ascending node (RAAN). This too involves a potentially expensive plane change maneuver. There are two ways of handling this: either a short duration mission to target objects whose RAANs align naturally, or a long duration mission where the maneuvering satellite can reside in an orbit that would allow for a differential drift in RAAN to accomplish the necessary plane change. It is assumed that the short duration mission must consist of impulsive burns while the long duration mission could consist of either impulsive or low thrust profiles. Both approaches will be considered in the following analysis.

The specific method used to compute the delta-V consisted of two independent steps. The first step was to determine the delta-V that would be required to match the slowly varying orbit elements when moving from one target to another. The second step was to consider the in-plane phasing necessary to perform rendezvous; this was computed assuming the slowly varying elements had already been matched. Boost and rendezvous were both included (one pair for each target) with one transfer orbit period between the two burns (Figure 6). Delta-V for proximity operations maneuvering was considered to be negligible. Note that the mission profile was not optimized; the goal of this study is delta-V sizing and optimization is best applied to specific missions. Based on proposed orbit maneuvering systems, the impulsive mission was assumed to have a total available delta-V of 1.8 km/sec while a low thrust mission was assumed to have 3.5 km/sec of delta-V. For the impulsive mission, if the orbit elements are examined separately, then sizing shows the delta-V of 1.8 km/sec can change the semi-major axis by 5600 km, eccentricity by 0.36, and inclination or RAAN by 14 deg.

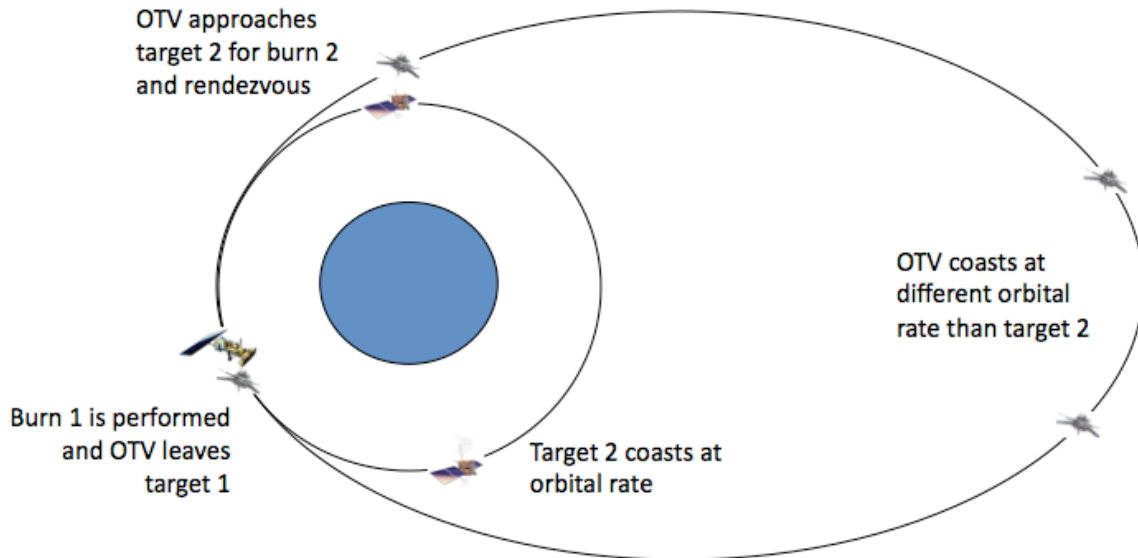


Figure 6: In-plane phasing maneuver burn plan

Five satellite groups were examined consisting of subsets of the possible targets from Table 1: 18 SL-16 rocket bodies (71 deg inclination, ~835 km altitude), 63 SL-8 rocket bodies (74 deg inclination, ~770 km altitude), 143 SL-8 rocket bodies (83 deg inclination, ~980 km altitude), 66 Iridium satellites (86 deg inclination, ~780 km altitude), and 10 SPOT bus satellites in Sun-synchronous orbit (~98 deg inclination, ~850 km altitude). These subsets were chosen as being likely targets within their larger orbital groups based upon considerations other than their orbits. The objects were kept to being the same type of structural object (i.e., all SL-16s, all SL-8s, all Iridium, all SPOT bus). This would make attachment technology and proximity operations protocol simpler, thus keeping the cost of the mission down. The Tselina-2 satellites that were deposited by the SL-16 rocket bodies were excluded as they are thought to be intelligence satellites, which politically would not be likely targets of ADR missions or any mission that would require close proximity operations.

Figures 7-11 depict the results for each group. Figure 7 shows the 18 SL-16 rocket bodies as a function of right ascension of ascending node (RAAN) at a given snapshot in time. All of these objects are in slightly different orbits from each other so the plot cannot be taken as a relative phasing that would be applicable at all times, but rather as a representative sample to show that multiple targets can be reached if the time of the mission is chosen appropriately. There were two groups of four objects each that could be reached for less than a total 1.8 km/sec of impulsive delta-V. Additional in-plane phasing for these two objects would require less than 0.2 km/sec. This limitation could be mitigated by using a long duration mission of several years in length, which would allow for a beneficial natural right ascension of ascending node drift between target orbits. However, for short-duration missions, the RAANs have to be closely lined up naturally to be able to rendezvous with as many desired targets as possible.

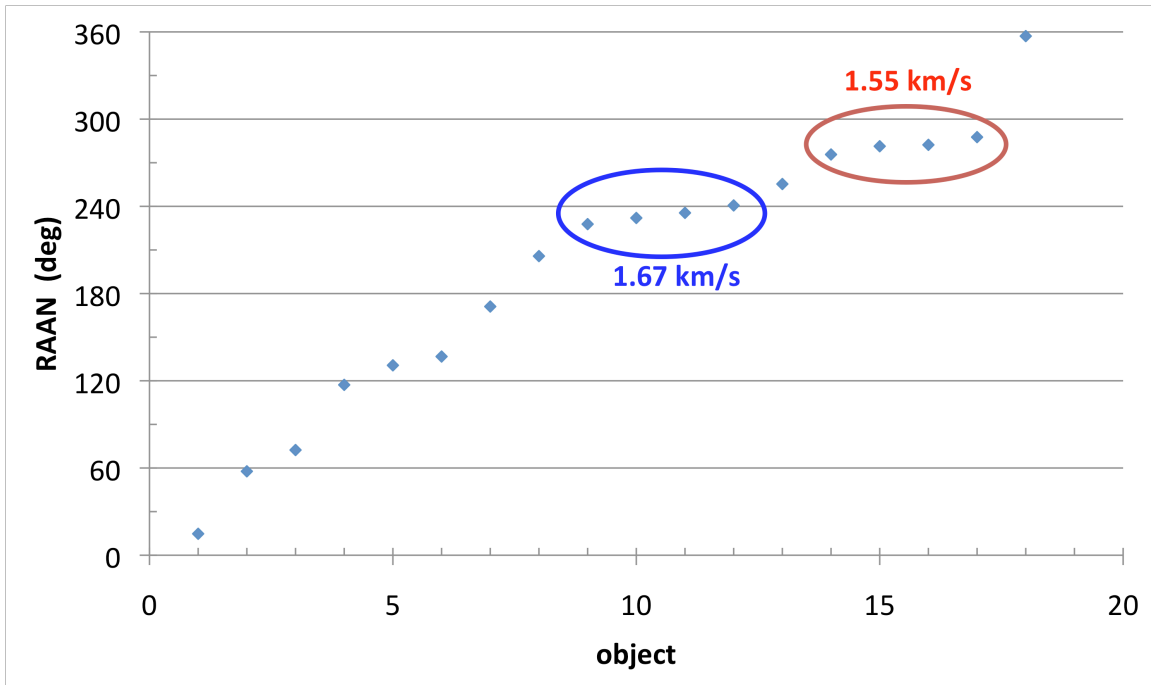


Figure 7: RAAN distribution for SL-16 rocket bodies

Figures 8 and 9 show a snapshot of the RAANs for the two inclination groups of SL-8 rocket bodies. There are multiple groups of 4 or more objects that can be orbit matched with total delta-V of less than 1.8 km/sec. For the 74 deg SL-8s, there were 5 separate groups that have chains where at least 4 objects within the chain would meet the 1.8 km/sec requirement (12 sequences of 4; 8 sequences of 5; 3 sequences of 6). For the 83 deg SL-8s, there are little restrictions on the objects and many opportunities to accomplish mission goals (109 sequences of 4; 95 sequences of 5; 80 sequences of 6). The in-plane phasing for the SL-8s would require less than 0.2-0.3 km/sec.

Figures 10 and 11 show the RAAN distribution for Iridium and the SPOT buses. For Iridium, orbit matching for the satellites within each plane would require ~ 0.06 km/sec of delta-V (negligible) and the in-plane phasing for 6 objects would require ~ 0.25 km/sec. Moving between the Iridium planes would require ~ 4.69 km/sec of delta-V, which is clearly too high to be viable for practical systems. For the SPOT buses, there were two groups of potential orbit matching sequences for this snapshot in time with either group requiring an in-plane phasing of ~ 0.2 km/sec. The first was Metop-A, Envisat, and Spot 4 (1.24 km/sec); the second was Envisat, Spot 4, Spot 5, and ERS-2 (0.95 km/sec). The important take-away from this part of the analysis is two-fold: 1) given realistic on-orbit maneuvering systems, there are groups of target vehicles that can be reached; 2) there is a limitation in which specific objects and the total number of objects that are reachable.

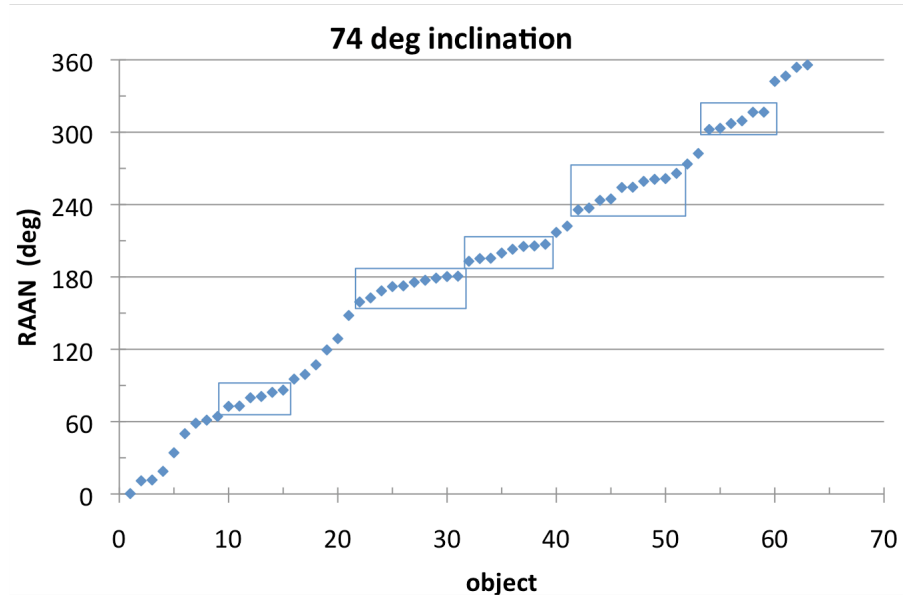


Figure 8: RAAN distribution for 74 deg inclination group of SL-8 rocket bodies

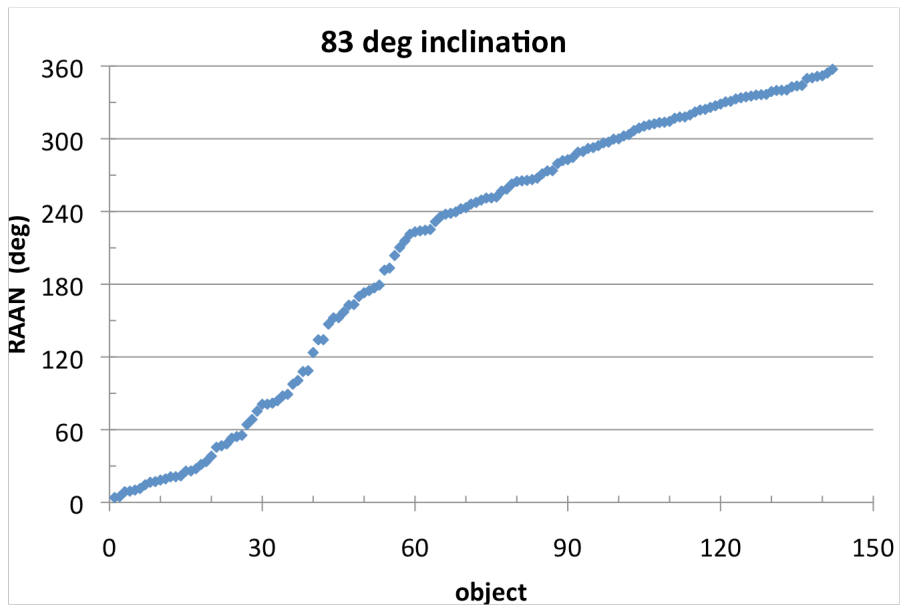


Figure 9: RAAN distribution for 83 deg inclination group of SL-8 rocket bodies

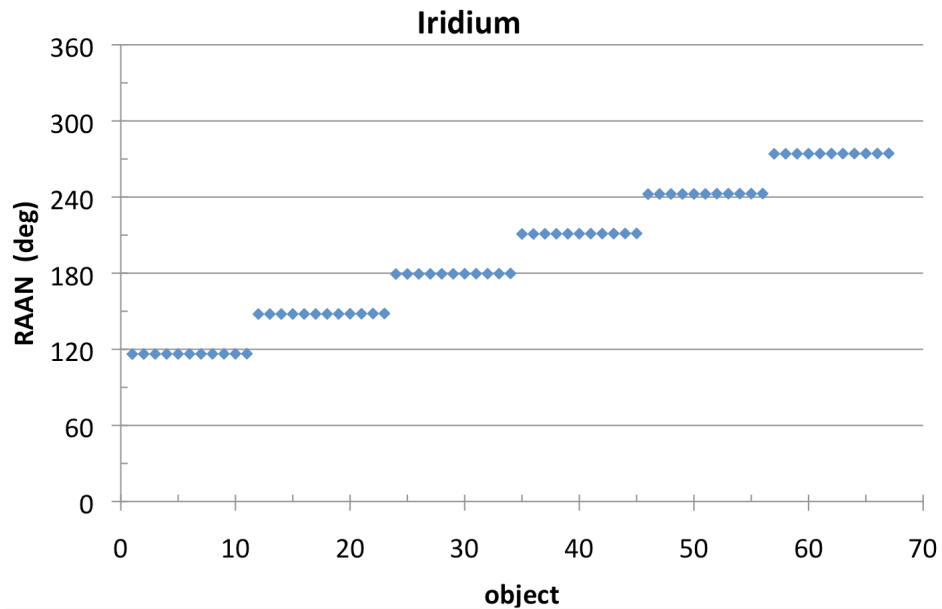


Figure 10: RAAN distribution for Iridium satellites

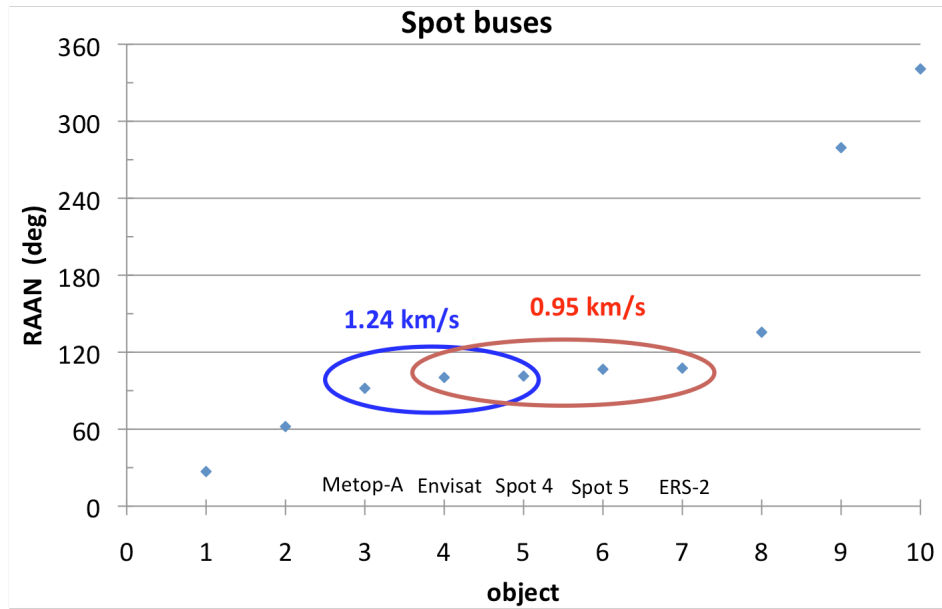


Figure 11: RAAN distribution for SPOT bus satellites

The second type of mission examined consisted of a multi-year mission that would potentially affect a large number of targets (20 targets was chosen as a realistic maximum for a single OTV) using either an impulsive or a low thrust system. Figures 12 and 13 show the difference in delta-V capability between the impulsive and low thrust (Edelbaum)^{7,8} options. The low thrust option assumed as a realistic OTV has more delta-V capability than the impulsive (3.5 km/s vs. 1.8 km/sec). But while the low thrust option does yield much greater capability in terms of in-plane changes (Figure 12), the limiting factor in reaching multiple targets is the required plane

change. For plane changes, the plane change capability for low thrust is slightly more effective than impulsive (18 deg vs. 14 deg; Figure 13).

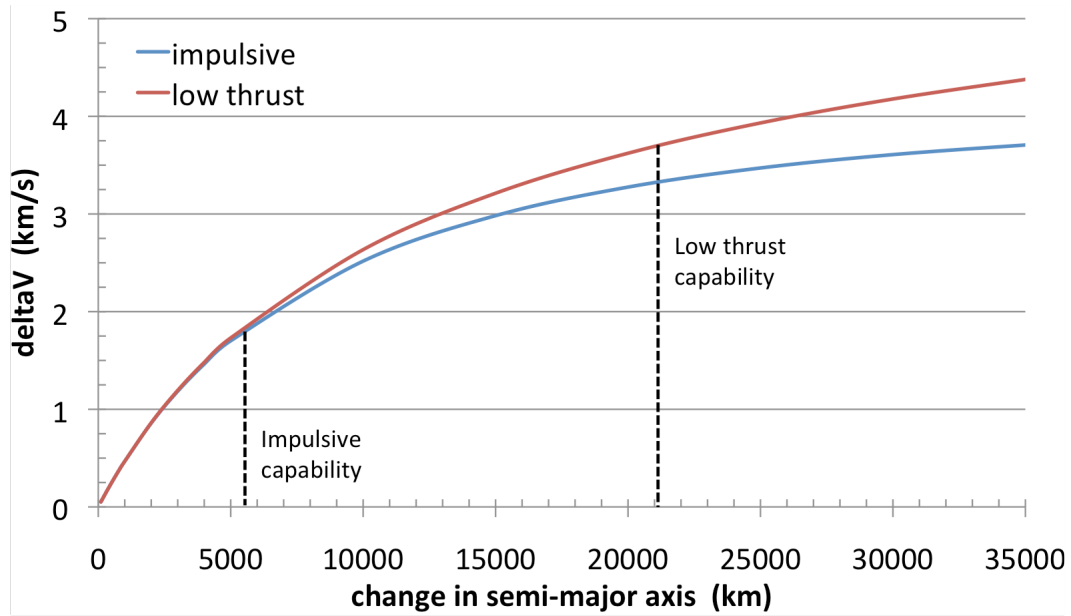


Figure 12: In-plane change performance capability of assumed impulsive and low thrust OTVs

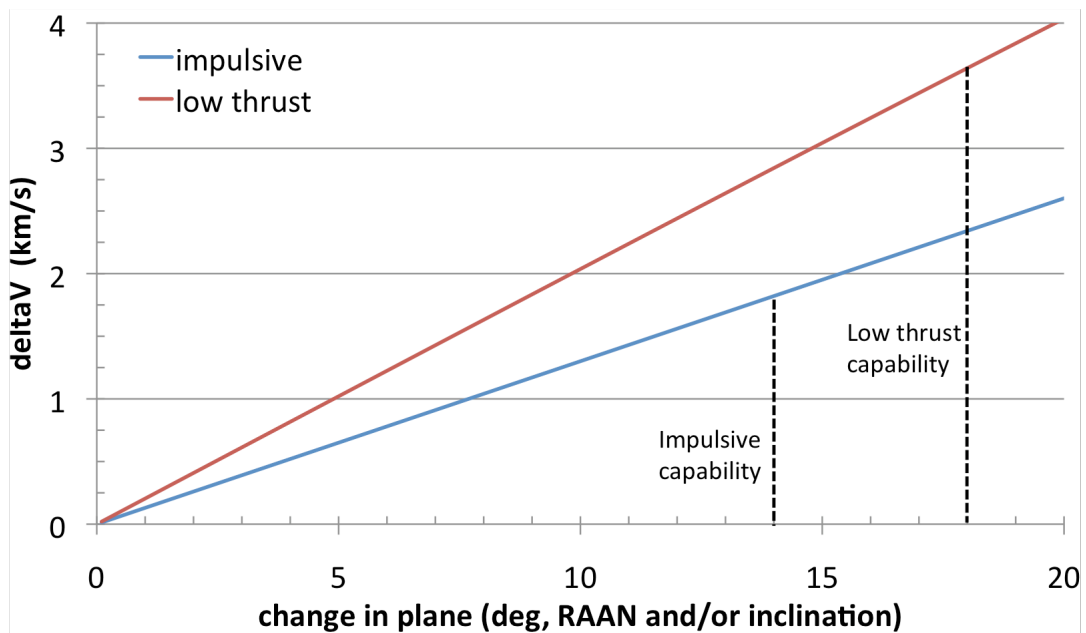


Figure 13: Plane change performance capability of assumed impulsive and low thrust OTVs

To avoid the large delta-Vs required for RAAN shifting, the OTV could save fuel by moving to an intermediate orbit and then letting the natural differential precession due to the Earth J_2 oblateness effect drift the RAAN over to the new position. The OTV would then match the other

orbit elements as usual. This up-drift-down profile would be repeated for each target until the delta-V capability is reached. Figure 14 shows the effect of semi-major axis change for various inclinations on the nodal drift with a baseline orbit altitude of 780 km. Most of the targets are in highly inclined orbits (74-99 deg); however, the drift in RAAN is more pronounced for lower inclined orbits. Note that the plot is symmetrical for inclinations greater than 90 degree and so only the 0-90 degree range is depicted. The high inclinations of the various target groups limit the applicability of this technique but still significantly open up the trade space. For example, using nodal drift for Iridium targeting will allow for shifting between 3 planes over 2 years and all 6 planes over 5 years if low thrust is used; using impulsive with nodal drift would allow access to 5 of the 6 planes over 5 years. If the goal is to reach up to 20 targets, then only one plane shift of ~32 deg is required for Iridium, and this is easily achievable. For the non-nodal drift case, the assumed delta-V capability did not allow for any shift between the Iridium planes. However, given the large inclination differences between the various target groups (Figure 15), moving between the groups is still prohibitive in terms of required delta-V.

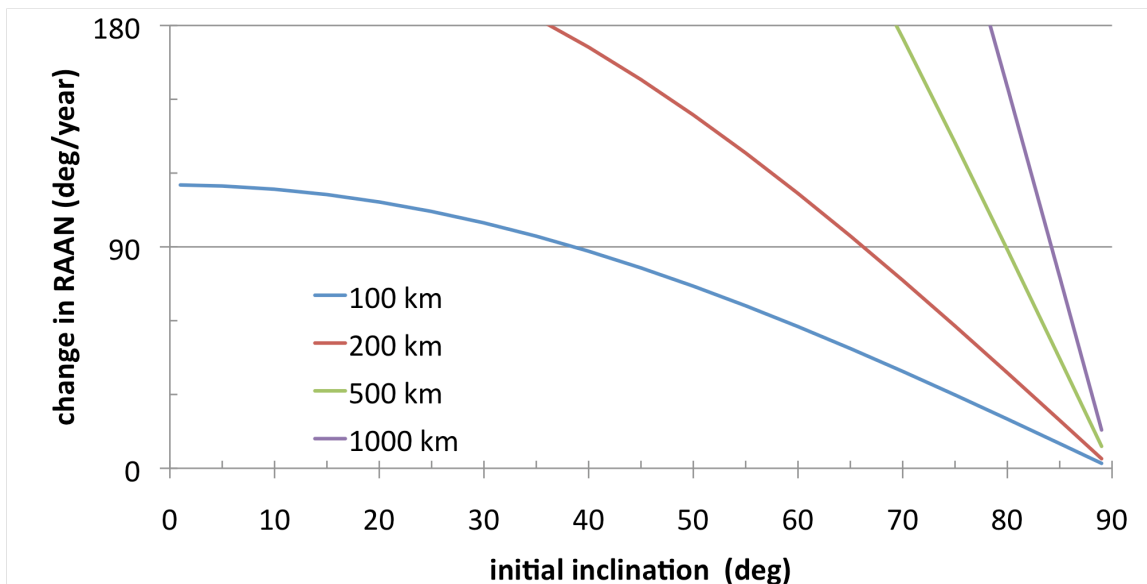


Figure 14: Relative nodal drift rates for various changes in semi-major axis

For the SPOT buses (Figure 11), the impulsive option including nodal drift over a 5-year mission allows for 6 of the 10 possible targets to be reached, an improvement of 2 over the non-nodal drift scenario while the low thrust option with nodal drift allows for 7 targets. For the SL-16 rocket bodies (Figure 7), there were 18 possible targets and only two groups of 4 could be reached without utilizing nodal drift. With nodal drift, the impulsive and low thrust options would allow for 9 and 10 targets respectively to be acquired. Both of these groups have less than 20 targets, but even so, the maximum number of targets achievable is less than the total (6 or 7 out of 10 for SPOT; 9 or 10 out of 18 for SL-16).

For the 74-degree SL-8 rocket body group, adding nodal drift to the process allowed for up to 14 and 11 targets to be reached by the low thrust and impulsive options for a 5-year mission. For the 83-degree SL-8 rocket body group, nodal drift allowed up to 15 and 12 targets for the low thrust and impulsive options. At first glance, the similar number of achievable targets between the two groups would appear to contradict Figures 8 and 9, which show that the 83-degree group has many more objects and hence the RAAN distribution is much denser than the 74-degree

group. However, due to the dependency of the nodal drift rate on the cosine of the inclination, the 74-degree group has a natural drift rate that is approximately 2.26 times the natural drift rate of the 83-degree group for objects at the same altitude. This allows the 74-degree group to have a much wider range of allowable RAANs for a similar number of targets than the 83-degree group. For example, the 74-degree group low thrust option reached 14 targets with a total RAAN change of 34 degrees while the 83-degree group low thrust option reached 15 targets with a total RAAN spread of 12 degrees.

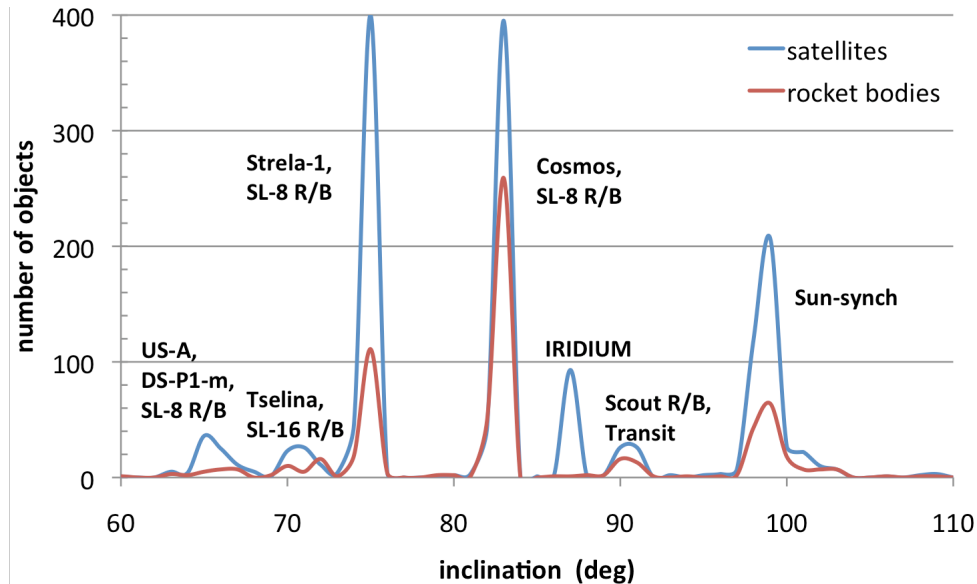


Figure 15: Inclination distribution of intact objects in LEO

6. Conclusion

The implications of this analysis are manifold. First, there is no way to know for certain which specific objects are going to cause a substantial increase in the future debris environment, so choosing desirable targets is based upon the probabilistic likelihood of objects contributing to the debris field. Modeling of the debris environment also shows that the most likely targets for ADR or tracking missions are in tightly constrained orbits, especially in the inclination, which limits the ability of a debris-related mission to move between targets that have different inclinations. Furthermore, targets should be selected in accordance with the presumed delta-V capabilities of the deploying vehicle. Given that the RAAN changes to an orbit are a limiting factor, using natural nodal drift to accomplish RAAN shifting enables a deploying vehicle to engage a larger number of targets, although potential target objects must still be in tightly defined inclination groups since moving between these groups is not feasible.

7. References

¹ A. B. Jenkin, M. E. Sorge, G. E. Peterson, J. P. McVey, B. B. Yoo, “100-Year Low Earth Orbit Debris Population Model,” *AAS 11-410*, AAS/AIAA Astrodynamics Specialist Conference, Girdwood, Alaska, August, 2011.

- ² G. E. Peterson, “Effect of Future Space Debris on Mission Utility and Launch Accessibility,” *AAS 11-414*, AAS/AIAA Astrodynamics Specialist Conference, Girdwood, Alaska, August, 2011.
- ³ W. Ailor, J. Womack, G. E. Peterson, E. Murrell, N. Lao, “Effects of Space Debris on the Cost of Space Operations,” 61st International Astronautical Conference, September 27, 2010, Prague, Czech Republic.
- ⁴ D. Sibert, D. Borgeson, G. E. Peterson, A. B. Jenkin, M. E. Sorge, “Operational Impact of Improved Space Tracking on Collision Avoidance in the Future LEO Space Debris Environment,” Advanced Maui Optical and Space Surveillance Technologies Conference, Maui, Hawaii, September 14-17, 2010.
- ⁵ J. C. Liou, “An Active Debris Removal Parametric Study for LEO Environment Remediation,” *Advances in Space Research*, Vol. 47, Issue 11, p 1865-1876, June 1, 2011.
- ⁶ J. W. Gangestad, S. A. Whalley, G. E. Peterson, “Orbital Constraints between Small Satellites and Communications Constellations,” *AAS 12-116*, 22nd AAS/AIAA Space Flight Mechanics Meeting, Charleston, SC, January 2012.
- ⁷ T. N. Edelbaum, L. L. Sackett, H. L. Malchow, “Optimal Low Thrust Geocentric Transfer,” *AIAA 73-1074*, AIAA 10th Electric Propulsion Conference, November, 1973.
- ⁸ J. A. Kechichian, “The Reformulation of Edelbaum’s Low-thrust Transfer Problem using Optimal Control Theory,” *Journal of Guidance, Control, and Dynamics*, vol. 20, no. 5, pp 988-994, 1997.